

Imaging the subsurface using acoustic signals generated by a vessel

Stian Hegna^{1*} investigates the use of the acoustic wavefield generated by a vessel for imaging the subsurface by estimating the emitted wavefield from the recorded direct arrivals, and discusses using this method with different acquisition configurations.

Abstract

The acoustic wavefield originating from a vessel has historically not been considered as a source of signal in the imaging of marine seismic data and is therefore treated as a source of noise. In this work, the feasibility of acquiring seismic data without an active source and instead using the acoustic wavefield generated by a vessel for imaging the subsurface has been investigated. There are areas around the world where the use of active marine seismic sources is not permitted throughout the year, or only permitted during short time periods. In such areas, acquiring seismic data using the acoustic signals generated by a vessel as a source may be an alternative. Using a vessel as a seismic source may also offer a low cost and low impact 4D monitoring solution with an opportunity for much more frequent acquisition of time lapse data especially over permanent receiver installations. This work demonstrates that it is possible to obtain very high-resolution seismic images of the shallow subsurface by using acoustic signals generated by a vessel. This outcome is due to the broadband signals that the vessel generates combined with the fact that these signals are generated continuously while the vessel is moving, allowing for extremely dense source-side sampling along the vessel path.

Introduction

Most vessels are designed to generate as little noise and vibrations in the hull as possible. However, it is well known that vessels are not silent and do generate an acoustic wavefield that interacts with the local subsurface geology. The resulting wavefield can be recorded using standard seismic sensors and data recording equipment.

Using recorded ambient noise for imaging the subsurface has been investigated by different authors who have suggested the use of a range of different methods and techniques. Seismic interferometry techniques, based on cross-correlating traces recorded in different positions, have been used to retrieve information about the subsurface without knowledge of the source wavefield. Different seismic interferometry approaches are discussed in Wapenaar *et al.* (2004). A different method using up-down deconvolution is described by Amundsen (2001). This is a method for eliminating the effect of the free surface from marine seismic

data in which the source wavefield is deconvolved as part of the process. A third method is referred to as imaging with separated wavefields, discussed in Whitmore *et al.* (2010). In common with up-down deconvolution, this method requires separated up- and down-going wavefields as input.

There are challenges with all the above-mentioned methods. To image the primary reflections without knowledge of the source wavefield, it is required that the complete wavefield emitted by the source that goes into the subsurface is recorded. The limited spatial coverage of receivers typically used in seismic survey geometries often means that a recording of the complete wavefield cannot be achieved.

Near-field hydrophones mounted close to individual source elements are commonly used for measuring the acoustic wavefield emitted by active seismic sources as proposed by Ziolkowski *et al.* (1982) and Parkes *et al.* (1984), and are standard equipment used in marine seismic data acquisition. Tests with a similar method, to investigate whether noise generated by propellers could be used as a seismic source, were discussed in Davies *et al.* (1992). The propeller signal was recorded with hydrophones protruded through the hull of a vessel just above the propeller. It is, however, unclear how well such recordings can characterize the overall acoustic wavefield generated by the vessel.

In this paper, a new method for deriving the vessel-generated acoustic wavefield using recorded direct arrivals, *a-priori* information about receiver positions, and an understanding of how the acoustic wavefield propagates from the source to the receivers, will be presented.

Method

The estimation of source signatures generated by airguns from recorded direct arrivals was described in Kravis (1985), by using a similar method as described in Ziolkowski *et al.* (1982) and Parkes *et al.* (1984) for determining source signatures from near-field measurements. The approach used in the work of these authors has similarities to the new method described here, since the estimation of the acoustic wavefield generated by a vessel is based on using the recorded direct arrivals. Firstly, the signals coming from the direction of the vessel, in other words the direct arrivals, are isolated as described in Hegna (2021). These

¹ PGS

* Corresponding author, E-mail: Stian.Hegna@pgs.com

DOI: 10.3997/1365-2397.fb2022093

isolated direct arrivals are backpropagated from the location of the receivers to the location from where the signals are emitted. Depending on the acquisition configuration, and in particular the positions of the receivers relative to the vessel, the location from where the signals are emitted may be determined from the data. If this is not possible due to the nature of the acquisition configuration, the location from where the acoustic signals are generated needs to be known. The acoustic wavefield generated by a vessel is likely to be a directional wavefield as discussed in Hegna (2022). Such a directional wavefield can be represented by a grid of point sources. The locations of these grid points need to be identified from the data; whether this is possible depends again on the acquisition configuration. Provided that these locations can be determined from the data, the directional wavefield can be estimated by isolating the signals emitted from each grid point and backpropagating these isolated direct arrivals from the locations of the receivers to the locations of the grid points. This is done in an iterative fashion starting with the location from where the strongest signals are emitted.

Once the origin of the strongest signals has been identified, the signals emitted from this grid point are estimated, the contributions of these signals to the recorded direct arrivals are determined and subtracted from the input data. In the following iteration the location where the strongest signals in the residual data are emitted from is identified, and the contribution of the signals from this point to the recorded direct arrivals are estimated and subtracted from the residual data from the previous iteration. The iteration loop continues until any new point source locations can no longer be identified, or the amplitudes of the residuals are not further reduced by additional iterations. The accuracy with which the grid point locations can be determined as well as the accuracy of the estimated acoustic wavefield depends on the acquisition configuration. The spatial sampling of the receivers as well as the x, y, z locations of the receivers relative to each source of acoustic energy are important factors.

Acquisition configurations

Three different acquisition configurations with different strengths and weaknesses will be discussed below; a typical single-vessel towed-streamer configuration, a configuration with a vessel

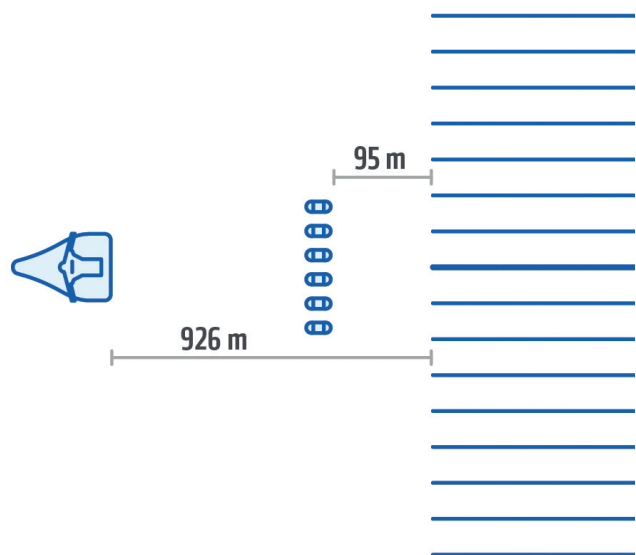


Figure 1 Towed-streamer acquisition configuration. The seismic vessel was towing 16 multisensor streamers with 100 m separation.

sailing over a towed-streamer spread, and a vessel sailing over a permanent reservoir monitoring (PRM) system installed on the seabed. The methodology presented here may be especially attractive in areas with PRM systems provided that the resulting data quality is sufficient. Field monitoring (4D) data could potentially be acquired with very low costs, minimal additional environmental footprint, and with short time intervals, since the PRM system may simply be turned on whenever any vessel is sailing over it.

Towed streamer

The estimation of the acoustic wavefield generated by a seismic vessel towing a streamer spread from the recorded direct arrivals, and the use of this wavefield for imaging the subsurface, was discussed in Hegna (2021). The acquisition configuration is shown in Figure 1.

When estimating the acoustic wavefield generated by the vessel towing such a large streamer spread, only a limited part of the acoustic wavefield (that is emitted from the vessel in the

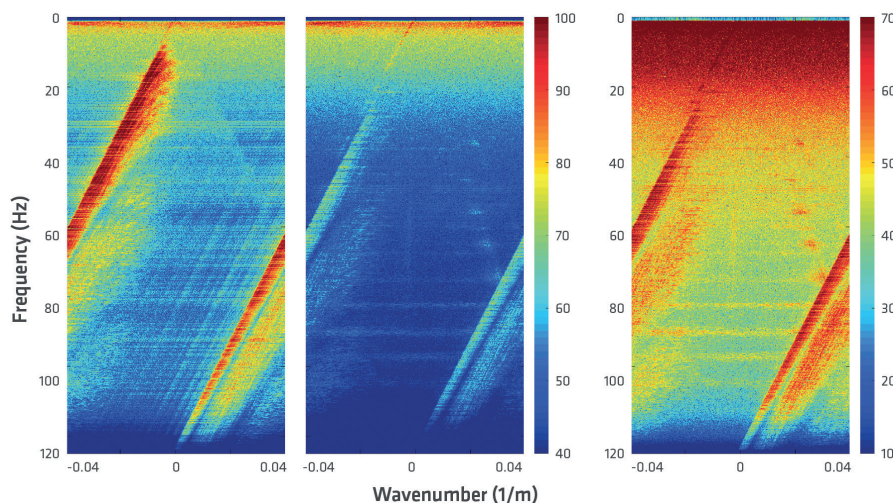


Figure 2 Frequency-wavenumber spectra of raw recorded hydrophone data when triggering airguns (left panel), and when recording data without using active sources (middle and right panels). In the panel on the right the limits of the colour scale have been compressed so that the acoustic signals appear more similar to the data acquired with an active source.

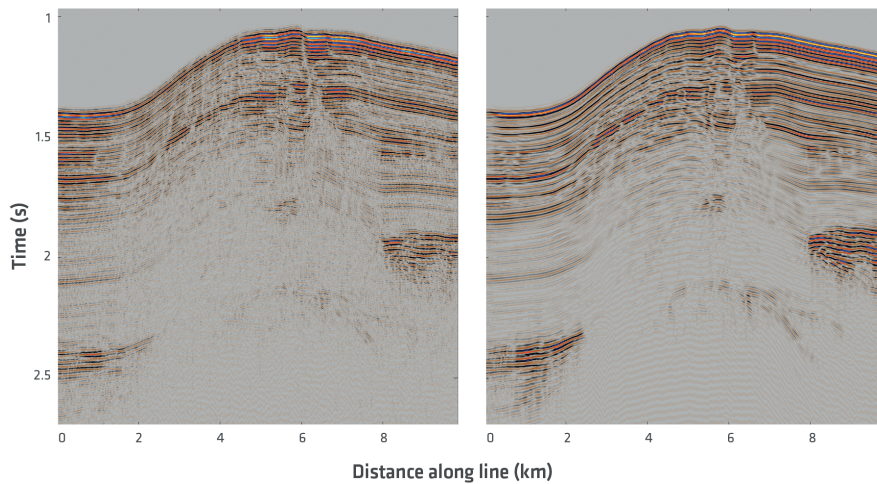


Figure 3 Comparison between a seismic image derived from data recorded without an active source using the acoustic signals generated by the seismic vessel as the source (left), and an image produced from data acquired by triggering individual airguns with short random time intervals (right).

direction towards the streamers towed far behind) is measured directly and can be characterized. Furthermore, since the recorded direct arrivals have propagated near-horizontally, the sea-surface reflection causes significant attenuation limiting the ability to estimate the emitted wavefield at the lowest frequencies. Figure 2 shows frequency-wavenumber spectra of data acquired with air guns, and of data acquired without triggering the air guns. Acoustic signals are clearly visible within the signal cone both in the data acquired with air guns sources and in the data acquired without an active source. When the colour scale of the spectrum derived from the data acquired without an active source is compressed such that the colours of the signals close to the edge of the signal cone that have propagated near horizontally are similar to those of the data acquired with an active source towards higher frequencies, the signals close to the edge of the signal cone are observed to have decayed more rapidly towards lower frequencies in the data acquired without an active source. This is due to the much longer horizontal distance between the vessel and the front of the streamers compared to the distance between the active sources and the streamer fronts. In addition, because the acoustic signals generated by the seismic vessel are much weaker compared to the signals emitted from the active sources, the signal-to-noise ratio is significantly lower in the data acquired without active sources especially towards the lower frequencies. As a result of the combination of these effects it is not possible to estimate the wavefield generated by the vessel below approximately 30 Hz with this configuration. Also, as the receiver arrays cause attenuation of the direct arrivals towards higher frequencies the wavefield cannot be estimated above approximately 125 Hz. Consequently, it is only possible to estimate the acoustic wavefield generated by the above-described acquisition geometry for a frequency range of 30 to 125 Hz.

A seismic image derived from towed-streamer data acquired without an active source compares well with an image produced from data acquired using air guns, as shown in Figure 3. However, the bandwidth of the resulting image is limited to between 30 and 125 Hz due to the factors discussed above. In addition to the limited bandwidth, the lack of near offsets means that such configurations are best suited to imaging the subsurface in deep water areas.

Vessel sailing over towed streamers

An alternative configuration where the vessel is sailing over the top of a streamer spread was discussed in Hegna (2022). The acquisition configuration is illustrated in Figure 4. The direct arrivals associated with the vessel that is sailing over the spread are measured over a much larger range of offsets and source emission angles compared to a traditional single-vessel towed-streamer configuration. Since the near-vertical part of the wavefield is measured directly, the acoustic wavefield generated by the vessel sailing on top of the streamer spread can be estimated over a large bandwidth including the low frequencies.

Figure 5 shows the time series and the amplitude spectrum of the pressure measurements recorded by the receiver group that is

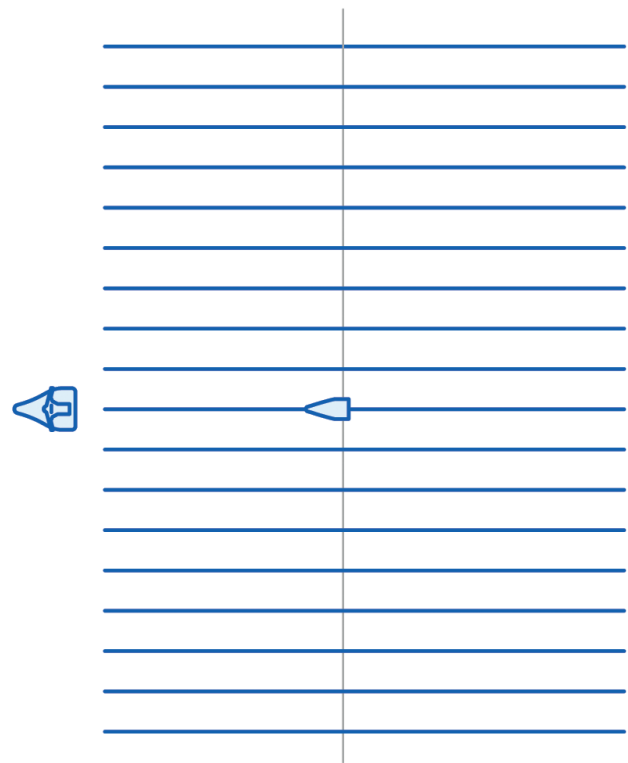


Figure 4 Acquisition configuration with a vessel sailing on top of the multisensor streamer spread. The seismic vessel in the front was towing 18 streamers with 75-m separation. The streamer depth was 30 m, and each streamer was 8 km-long.

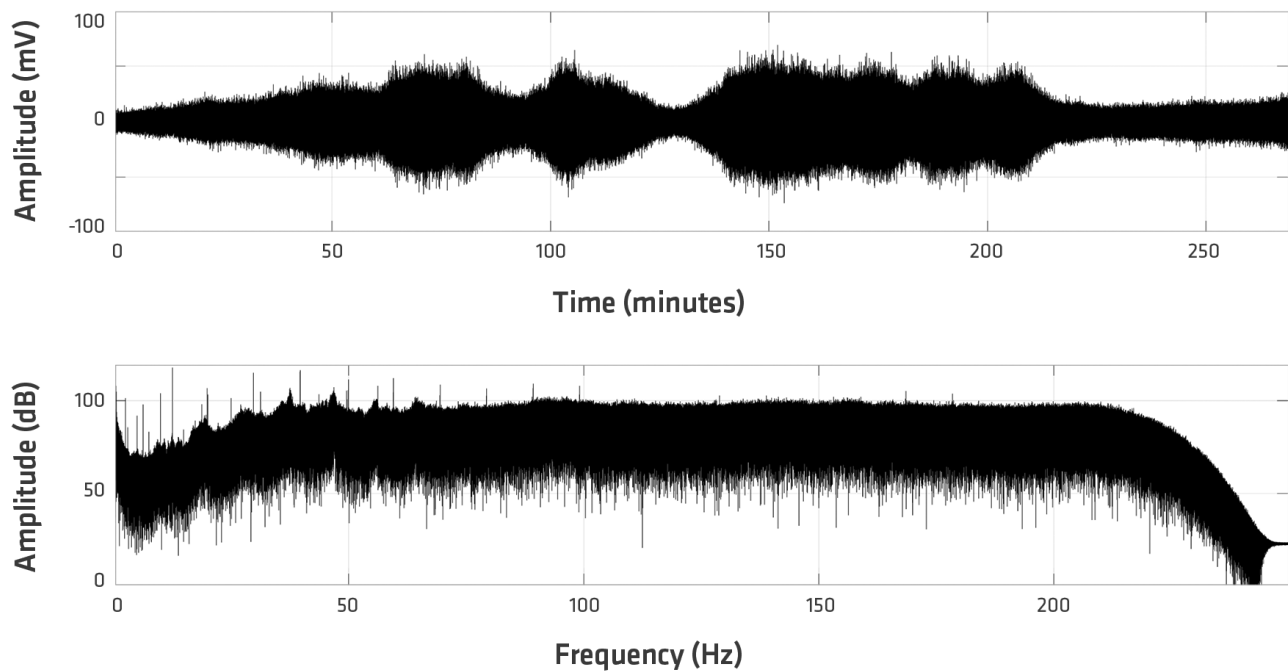


Figure 5 Time series (upper graph) and amplitude spectrum (lower graph) of raw recorded hydrophone data recorded on channel 281 in streamer 10 which was on average closest to the vessel position.

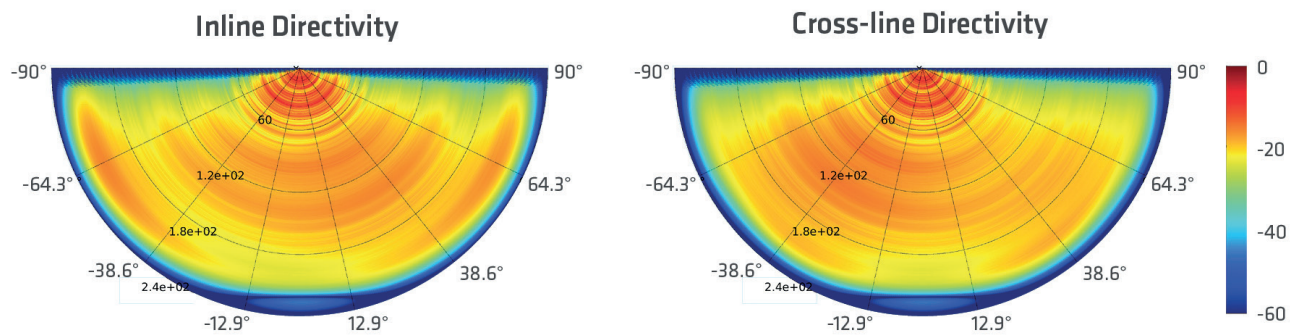


Figure 6 The inline (left) and crossline (right) directivity of the emitted acoustic wavefield from the vessel sailing on top of the streamer spread. The emission angles range from -90 to 90 degrees and the displayed frequency range is from 0 to 240 Hz (the wavefield has been estimated up to 250 Hz).

closest to the location of the vessel sailing above the streamers. The amplitude spectrum shows that the acoustic signals generated by the vessel contains a very broad range of frequencies limited only by the anti-alias filter of the recording system.

Figure 6 illustrates the directivity of the estimated wavefield generated by the vessel sailing over the streamer spread. The wavefield appears to be mostly omnidirectional; it does not contain any deep notches in any particular direction and exhibits only minor variations with emission angle.

Figure 7 shows a comparison between NMO stacks derived from data using the vessel as the source and by triggering air gun arrays. The NMO stack of the data acquired with an active source is a QC stack from an early pre-processing step and does not show the full potential of the data. However, this comparison shows that the main features observed in the data acquired when using an active source can also be recognized in the data acquired when using the vessel as a source. This figure also illustrates the resolution that can be achieved in the shallow section when using acoustic signals generated by a vessel, and with this specific

configuration. The use of a continuous source wavefield, rather than discrete shot points, is likely a significant contributory factor to the high spatial resolution. The broadband acoustic signals generated by the vessel in combination with the robust removal of the receiver ghost with multisensor streamers are likely to be the main contributory factors to the high temporal resolution.

The upper part of Figure 8 shows the NMO stack of the data acquired when using the vessel signal from a different part of the line, that further illustrates the high resolution that can be achieved. The octave panels in the lower part of Figure 8 show that the bandwidth of the resulting NMO stack covers seven octaves in the shallow section with coherent signals demonstrated from the 2-4 Hz octave all the way up to 250 Hz.

Vessel sailing over a PRM system

To test the feasibility of the method described here for reservoir monitoring applications without having access to real PRM data, such data had to be simulated. The receiver layout shown to the left in Figure 9 consists of five 1200m-long cables with 300 m

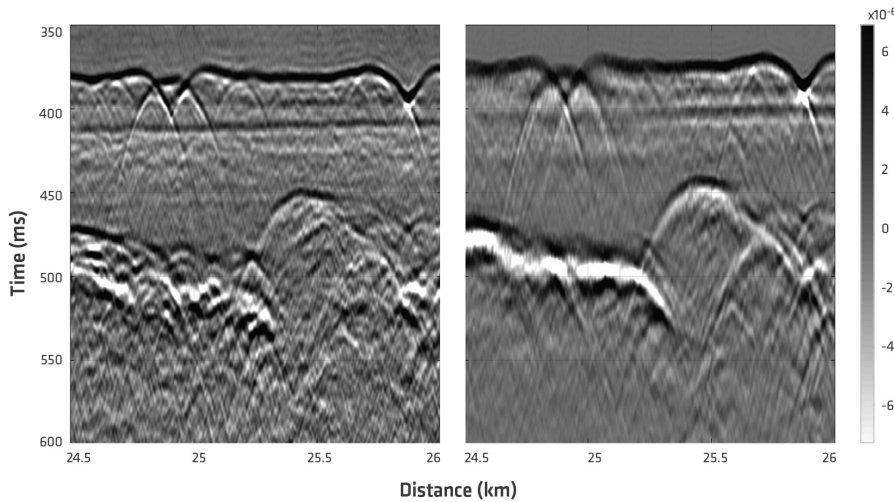


Figure 7 NMO stack from data acquired without an active source (left) and with air gun arrays (right).

spacing, and 50 m receiver interval along each cable. The water depth and the receiver depth are 400 m. The simulated source wavefield is band-limited white noise covering a frequency range from 0.5 to 125 Hz. The source is moving with a constant speed of 2.5 m/s over the central cable with all sensors recording continuously. The geological model consists of a horizontal water bottom at 400 m with a reflection coefficient of 0.4, and a single horizontal reflector at a depth of 450 m with a reflection coefficient of 0.3. The direct arrival, as well as the reflected signals and the surface-related multiples for both pressure as well as three component velocity sensor measurements, have been simulated. A short time window of the simulated hydrophone data is shown to the right in Figure 9.

The emitted wavefield has been estimated using the method outlined above. With a towed-streamer configuration where the streamers and the vessel follow each other, the relative

distances between the vessel and the receivers change slowly. Therefore, the same operators describing the propagation of the emitted wavefield to the locations of the receivers can be used over time windows that are of the order of 10-20 s long without compromising the accuracy of the wavefield estimation. With stationary receivers and a vessel that is continuously moving over the receivers, the relative distances between the vessel and the receivers are continuously changing. Therefore, the operators describing the propagation of the emitted wavefield to the receivers are also continuously changing.

The degree to which the direct arrivals can be isolated from the recorded data depends on the spatial sampling of the receivers. The relatively large receiver spacing that is typical for PRM systems may lead to leakage of signals that are not associated with the direct arrivals due to spatial aliasing. Also, compared to the case where a vessel is sailing over a streamer spread, the

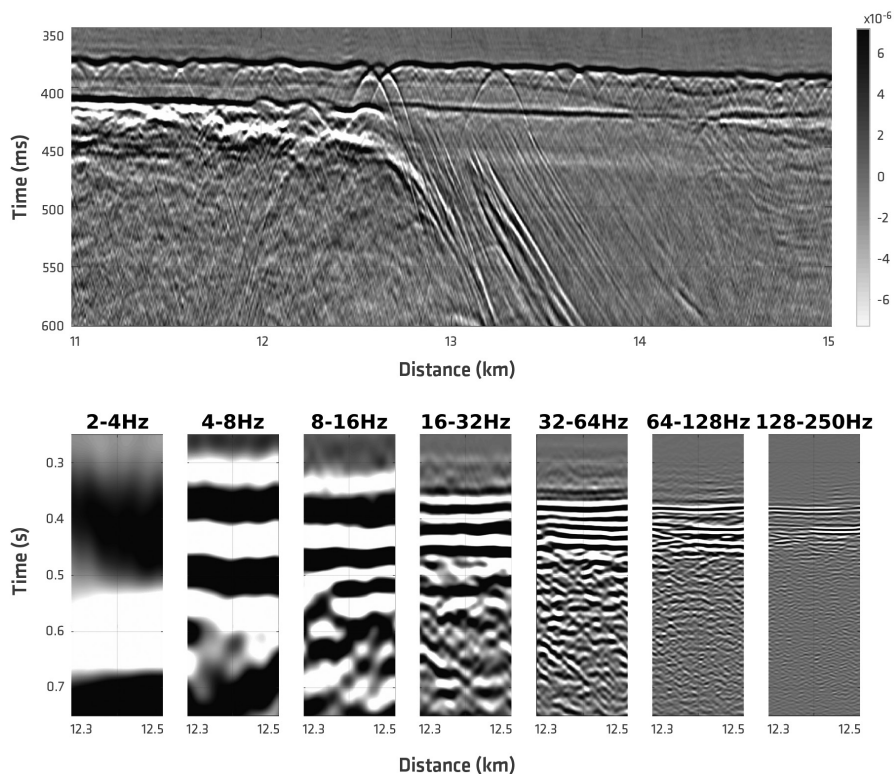


Figure 8 The NMO stack of the data acquired without an active source from a different part of the line (upper image), and octave panels from parts of the same NMO stack (lower image).

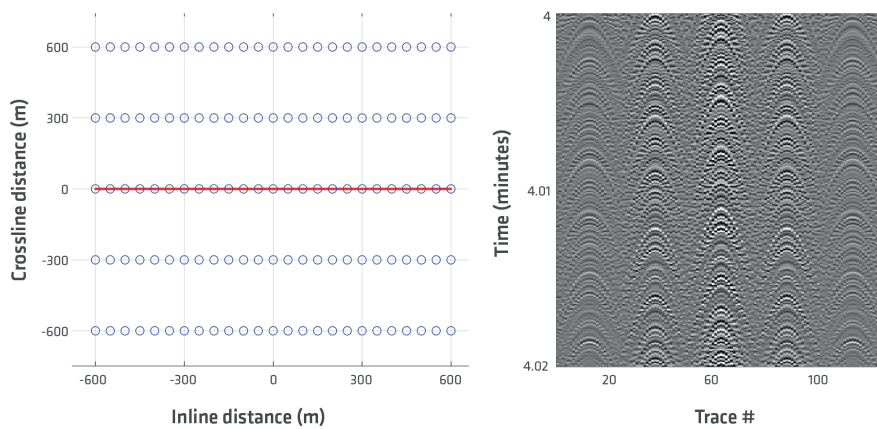


Figure 9 Source and receiver layout used for simulating PRM data (left), and portions of simulated hydrophone data (right). The blue circles are receiver positions, and the red line shows the sail line position for the vessel sailing over the PRM system with a constant speed of 2.5 m/s.

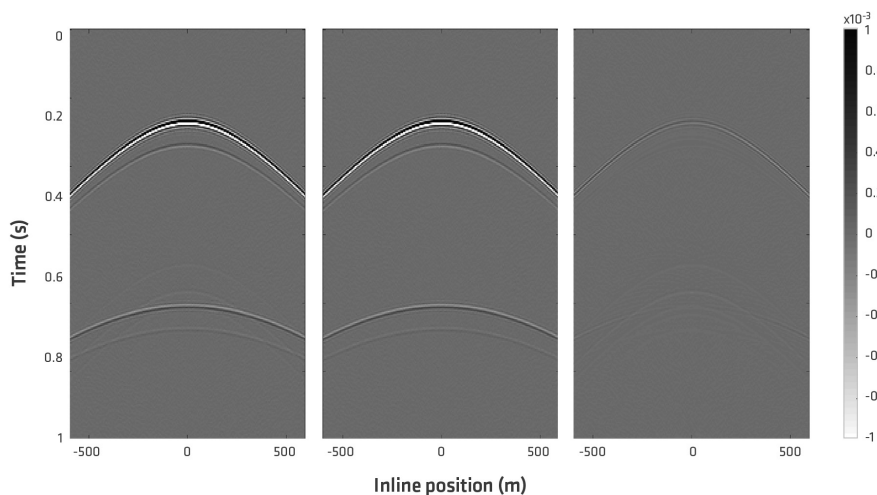


Figure 10 Common receiver gather after deconvolving the estimated source wavefield (left) from the synthetic hydrophone data with a PRM system, after deconvolving the actual source wavefield used to generate the synthetic data (middle), and the difference between the two results (right).

larger vertical distance between the vessel and receivers located on the seafloor makes the direct arrivals less dominant compared to other signals in the received data in the area closest to the vessel. Leakage of signals not associated with the direct arrivals can, however, be reduced by using both the pressure and the three component particle velocity measurements in combination. By performing a time-variant vector rotation of the three component measurements such that one component always points in the direction directly towards the vessel during the entire time of the data recording, a scaling to compensate for sensitivity and acoustic impedance, and summing the component pointing towards the source with the pressure measurements, the down-going pressure field coming from the direction of the vessel can be derived. This down-going pressure field is used as input data for the estimation of the acoustic wavefield generated by the vessel.

Figure 10 compares common receiver gathers after deconvolving the estimated and true source wavefields from the simulated hydrophone data. Since a vessel emits signals continuously, the spatial sampling of the receiver gathers after the deconvolution can be chosen. In this case the chosen trace spacing is 6.25 m to ensure no spatial aliasing up to 120Hz. The results exhibit only minor errors that are mainly related to imperfect isolation of the direct arrivals in the simulated PRM data.

This synthetic study indicates that it is possible to estimate the acoustic wavefield generated by a vessel sailing over a PRM system with sufficient accuracy to retrieve impulse responses of the subsurface beneath the PRM system.

Conclusions

It has been shown that imaging the subsurface using the acoustic wavefield generated by a vessel is feasible and that high resolution images can be obtained with certain acquisition configurations. Three different configurations have been considered; a towed-streamer configuration, a configuration with a vessel sailing over the top of a towed-streamer spread, and a configuration with a vessel sailing over a PRM system.

The single-vessel towed-streamer configuration using the acoustic wavefield generated by the seismic vessel towing the streamers for imaging the subsurface gives results that compare well with seismic data acquired using air guns. There are, however, limitations with this configuration due to the large horizontal distances between the vessel and the receivers. This means that the resulting image is limited in bandwidth to between 30 and 125 Hz.

The second configuration with a vessel sailing on top of a streamer spread shows excellent results. Due to the much improved near-offset coverage and recording of direct arrivals over a much larger range of emission angles, the acoustic wavefield generated by the vessel can be determined with higher precision over a much wider bandwidth. This results in excellent broadband images; coherent signals have been demonstrated from the 2-4 Hz octave all the way up to 250 Hz in the shallow parts of the section.

The third configuration considered is a vessel sailing over a PRM system. Due to lack of access to real PRM data, synthetic

data using a simple geological model have been created. Despite the challenges related to the coarse sampling of receiver locations, the synthetic experiment indicates that the method will work well with PRM systems. The results after deconvolution of the estimated source wavefield from the received wavefield look promising with only minor errors mainly related to imperfect isolation of the direct arrivals in the simulated PRM data.

Acknowledgements

We would like to thank to Lundin Energy Norway AS and its partners DNO Norge AS and Petoro AS in PL1083 for permission to show the results from the test with a vessel sailing on top of the streamer spread.

We would also like to thank PGS for supporting this work and for permission to publish the results.

References

- Amundsen, L. [2001]. Elimination of free-surface related multiples without need of the source wavelet. *Geophysics*, **66**, 1.
- Davies, K., Hampson, G., Jakubowicz, H. and Odegaard, J. [1992]. Screw seismic sources. 62nd Annual International Meeting, SEG, Expanded Abstracts, 710-711.
- Hegna, S. [2021]. Continuous wavefields method – The acoustic wavefield generated by the seismic vessel. 82nd Conference and Exhibition, *EAGE*, Extended Abstracts, 2021, 1-5.
- Hegna, S. [2022]. The acoustic wavefield generated by a vessel sailing on top of a streamer spread. 83rd Conference and Exhibition, *EAGE*, Extended Abstracts, 2022, 1-5.
- Kravis, S.P. [1985]. Estimation of marine source signatures from direct arrivals to hydrophone groups. *Geophysical Prospecting*, **33**, 987-998.
- Parkes, G.E., Ziolkowski, A., Hatton, L. and Haugland, T. [1984]. The signature of an air gun array: Computation from near-field measurements including interactions – Practical considerations. *Geophysics*, **49**, 105-111.
- Wapenaar, K., Draganov, D., van der Neut, J. and Thorbecke, J. [2004]. Seismic interferometry: a comparison of approaches. 74th Annual International Meeting, SEG, Expanded Abstracts, 1981-1984.
- Whitmore, N.D., Valenciano, A.A., Sollner, W. and Lu, S. [2010]. Imaging of primaries and multiples using a dual-sensor towed streamer. 80th Annual International Meeting, SEG, Expanded Abstracts, 3187-3192.
- Ziolkowski, A., Parkes, G.E., Hatton, L. and Haugland, T. [1982]. The signature of an air gun array: Computation from near-field measurements including interactions. *Geophysics*, **47**, 1413-1421.